ELSEVIER

Mechanisms of Development 88 (1999) 159–172

www.elsevier.com/locate/modo

Induction of apoptosis in the germline and follicle layer of *Drosophila* egg chambers

Sheng-Hao Chao, Rod N. Nagoshi*

Department of Biological Sciences, University of Iowa, Iowa City, IA 52242-1234, USA

Received 12 April 1999; received in revised form 13 July 1999; accepted 23 July 1999

Abstract

The *reaper* and *head involution defective* genes can induce apoptotic death in several *Drosophila* cell types, including portions of the embryo and eye. By a combination of *FLP* recombinase and the yeast *Gal4/UAS* transcription activation system, we expressed both cell death genes in discrete clones in the adult ovarian follicle cell layer. The expression of either *reaper* or *head involution defective* induced follicle cell apoptosis during all oogenic stages. Unexpectedly, the disruption of the follicle layer led to the induced degeneration of the nurse cells in an apoptotic manner, demonstrating a germline-somatic interaction required for germ cell viability. The germline apoptosis initiates at a specific time in oogenesis, coinciding with the beginning of vitellogenesis. This observation is intriguing given previous suggestions of a process to eliminate defective egg chambers at these same oogenic stages. The induce germline degeneration initiates with the transient formation of a network of filamentous actin around the nurse cell nucleus, in close association with a product of the adducin-related *hu-li tai shao* gene. This was immediately followed by nuclear condensation and DNA fragmentation, both characteristics diagnostic of apoptosis. Occurring concomitantly with the nuclear phenotypes were the disorganization of ring canals, and the degradation of Armadillo protein (a β-catenin homolog) and filamentous actin. Germ cells degenerating as a normal consequence of oogenesis displayed a similar set of phenotypes, suggesting that a common apoptotic mechanism may underlie these different germline death phenomena.

Keywords: Programmed cell death; Reaper; Head involution defective; Oogenesis; Nurse cells

1. Introduction

Programmed cell death (PCD), or apoptosis, denotes a regulated process of cell suicide (reviewed in Hengartner, 1994; Vaux and Korsmeyer, 1999). Death results from a cell autonomous and physiological mechanism triggered by intrinsic signals or external stimuli. PCD has been observed in a number of systems and is essential for the removal of supernumerary, deleterious, or defective cells. An essential characteristic of PCD is that death occurs through an orderly and stereotypic sequence of cytological events. Perhaps most diagnostic are the nuclear aberrations that typically occur early in the process, including nuclear condensation and internucleosomal cleavage of DNA (Wyllie et al., 1980; Duke et al., 1983). Other common characteristics are early cell contraction and plasma membrane blebbing, followed by localized phagocytotic removal of the dying cells (Kerr et al., 1972; Ellis et al., 1991; Deckwerth and Johnson, 1993). Relatively little is known about the molecular mechanisms underlying many of the observed nuclear and cytoplasmic apoptotic events. For example, it is not clear what cytological processes are required for nuclear condensation and how this morphological aberration might be related to DNA fragmentation.

In *Drosophila melanogaster*, several genes involved in PCD have been identified (reviewed in McCall and Steller, 1997). Among the best characterized of the activators of apoptosis are *reaper* (*rpr*) and *head involution defective* (*hid*) (White et al., 1994; Grether et al., 1995; White et al., 1996). RNA from *rpr* is expressed in a subset of cells that are fated to die and the ectopic expression of *rpr* in embryos or the eye can cause increased apoptotic death. An analogous set of results was found with the *hid* gene (Grether et al., 1995). Although their mechanism of action is not completely known, both *rpr* and *hid* are likely to be components of a more general cell death mechanism (reviewed in Bergmann et al., 1998). The apoptosis induced by *rpr* and *hid* can be blocked by the baculovirus p35 protein, a general inhibitor of the ICE/CED-3 proteases,

* Corresponding author. Tel.: +1-319-335-1076; fax: +1-319-335-1069.

E-mail address: rodney-nagoshi@uiowa.edu (R.N. Nagoshi)

0925-4773/99/$ - see front matter
PII: S0925-4773(99)00183-5

also called caspases (White et al., 1994; Grether et al., 1995; Nordstrom et al., 1996).

We are interested in examining the biology of PCD-like processes during *Drosophila* oogenesis, which have certain advantages for the study of developmental processes. The ovary consists of two lobes, each containing 15–20 linear structures called ovarioles (King, 1970; Spradling, 1993). Germline cystoblasts are located at the distal tip of the ovariole in a region known as the germarium. These undergo four mitotic divisions to generate 16 cystocytes connected by intercellular bridges called ring canals. One cystocyte becomes the oocyte while the other 15 differentiate into large, polyploid nurse cells that function to produce and transport maternal factors into the oocyte. At the 16 cystocyte stage, somatic follicle cells surround the germline syncytium to form the egg chamber. The subsequent maturation of the egg chamber has been organized into discrete stages on the basis of morphological criteria (King et al., 1956). Stage 1 chambers represent the 16 cell syncytium immediately after encapsulation by the follicle cells, while at stage 14, the nurse cells have degenerated and the mature oocyte extends throughout the chamber. Because oogenesis occurs continually in the adult, each ovariole contains a developmental sequence of egg chambers, with the youngest cysts near the germarium and more mature chambers at the posterior oviduct. This morphological arrangement greatly facilitates studies examining the temporal sequence of germline biological processes.

Apoptotic-like death of the nurse cells occur late in oogenesis as a normal consequence of egg chamber development. In stage 10 egg chambers, there is a rapid transfer of cytoplasmic contents from the nurse cells to the oocyte, a process known as cytoplasmic 'dumping.' Shortly thereafter, the depleted nurse cells become sequestered in the anterior tip of the egg chamber and rapidly degenerate, displaying both DNA fragmentation and nuclear condensation (Foley and Cooley, 1998). Interestingly, it is during this period that *dcp-1* is required in oogenesis (McCall and Steller, 1998). *dcp-1* encodes for the *Drosophila* caspase homolog, a protease required for apoptotic death. Germ cells mutant for *dcp-1* develop to stage 10, but fail to undergo dumping and show delayed nurse cell degeneration. Although *rpr* and *hid* RNAs are expressed during this period, neither gene is required in the germline for the death of the nurse cells or for oogenesis in general (Foley and Cooley, 1998).

In this paper, we demonstrate that the somatic follicle cells are sensitive to *rpr*- or *hid*-induced apoptotic death, which can be suppressed by the simultaneous expression of the baculovirus p35 protein. Substantial cell death in the follicle layer leads to the degeneration of the germline nurse cells, which also appears to occur by an apoptotic process. While the follicle cells could be killed during most oogenic stages, nurse cell death only became apparent during and after stages 7–8. Therefore, compromises in the integrity of the follicle layer leads to stage-specific nurse cell degeneration. This induced germ cell death provides a powerful system for examining the cytological events associated with apoptosis. For example, we observed that the death of the nurse cells began with the accumulation of filamentous actin (f-actin) and a product of the *hu-li tai shao* (*hts*) gene around the nurse cell nucleus. This event directly preceded the extensive nuclear aberrations that are normally among the earliest symptoms of apoptotic death. Comparisons with nurse cell death observed in wildtype ovaries, either as a result of normal maturation or due to environmental stress, suggest a common apoptotic mechanism occurring in each instance. These data support the proposal that there exists an active process to eliminate defective chambers in wildtype ovaries.

2. Materials and methods

2.1. Fly stocks and culture

The following transgenic lines are marked by the wildtype allele of the *white* gene, w^+. *GMR-Gal4* places *Gal4* under the control of the eye-specific *glass* enhancer (M. Freeman, from the Bloomington *Drosophila* Stock Center). *hs-FLP* places the yeast *FLP*-recombinase under the control of the *hsp70* promoter (from K. Golic). The *Act* > *CD2* > *Gal*4 construct places *Gal4* under the control of the *Actin5C* promoter (Pignoni and Zipursky, 1997). Between the promoter and *Gal4* gene lies a *CD2* transcriptional stop sequence that blocks *Gal4* expression, flanked by two *FRT* sites in direct orientation. FLP-induced site-specific recombination at these *FRT* sites would lead to the loss of the *CD2* transcriptional stop, allowing expression of *Gal4* from the actin promoter. *UAS-lacZ* places the bacterial *lacZ* gene under the control of the yeast *UAS cis*-acting transcriptional regulatory sequence (Brand and Perrimon, 1993). Binding of GAL4 to the *UAS* site will induce expression from *lacZ*.

Flies were raised on a standard cornmeal, molasses, yeast, agar media containing propionic acid as a mold inhibitor. Unless otherwise noted, alleles and chromosomes used are described in Lindsley and Zimm (1992). All crosses were cultured at either room temperature (20–23°C) or in a 25°C incubator. To optimize oogenic development, all crosses were supplemented with live yeast.

2.2. Generation of constructs and transgenic flies

The *UAS-rpr* transgene was created by isolating the complete *rpr* cDNA sequences from *p13B2* using *Xba*I and *Xho*I (White et al., 1994). The *rpr* fragment was inserted in the appropriate orientation into p*UAS*T. *pUAST* contains a polylinker flanked $5'$ by five tandem copies of the *UAS* regulatory element and $3'$ by an *SV40* polyadenylation site, all in a w^+ *P*-element transformation vector (Brand and Perrimon, 1993). The *hid* cDNA was isolated by *Eco*RI digestion and subcloned into *pUAST* to form *UAS-hid*

(Hay et al., 1994; Hay et al., 1997). The correct orientation of the *hid* sequence was determined by *Xba*I digestion. The *pRS* construct (Genbank accession number M16821) contains the entire *p35* open reading frame (ORF) and a portion of the *p94* ORF (Hay et al., 1994; Hay et al., 1997). To isolate the *p35* ORF, *pRS* was linearized with *Nru*I that separates the *p35* and *p94* sequences. *Eco*RI linkers were ligated to blunt ends and the fragment digested with *Eco*RI. A 1.1 kb fragment was isolated carrying the entire *p35* coding region and subcloned into *pUAST*. Constructs with *p35* in the appropriate orientation were identified by digestion with *BamH*I and *Bst*XI.

Transgenic lines were generated by standard *P*-element transformation methods (Ashburner, 1989), using either the *Δ2-3* plasmid or fly strain as a transposase source. The transgenic lines isolated and used in this study include: *UAS-rpr* on the *X* chromosome, *UAS-p35* on the third chromosome, and *UAS-hid* on the third chromosome balancer *TM6, Ubx*.

2.3. Generation of Gal4-expressing clones in the ovary

The *FLP/FRT* site-specific recombination method was used to generate follicle cell clones in egg chambers. Females were generated of the following genotypes: (1) *Act > CD2 > Gal4/+*; *UAS-lacZ/hs-FLP*, (2) *UAS-rpr/ Act > CD2 > Gal4*; *UAS-lacZ/hs-FLP*, (3) *Act >CD2Gal4/-Gal4/+*; *UAS-lacZ/hs-FLP*; *UAS-hid/+*, (4) *UAS-rpr/ Act>CD2>Gal4*; *UAS-lacZ/hs-FLP*; *UAS-p35/+*. These females were aged 3–7 days and heat shocked at 37°C for 1.5–2 h. The ovaries were dissected and analyzed at various times after heat shock (as indicated in text). The females were supplemented with live yeast and paired with males both before and after heat shock treatment.

2.4. Whole mount immunohistochemistry and fluorescent labeling

Adult gonads were dissected in PBS (130 mM NaCl, 7 mM Na_2HPO_4-$2H_2O$, 3 mM NaH_2PO_4–$2H_2O$). The tissues were fixed in a 1:1 solution of fix:heptane (fix: 4% paraformaldehyde in PBS) for 20 min with gentle agitation. The tissues were washed four times in PBT (0.1% Triton X-100, 0.05% Tween 80 in PBS) for 15 min each. Tissue preparations were permeabilized for at least 2 h in PBT + 1 mg/ml crystalline bovine serum albumin (BSA, Sigma) at room temperature. Primary antibodies were diluted in the PBT/BSA solution and incubated at 4°C overnight. Secondary antibodies were diluted 1:200 in PBT + BSA and incubated with tissues for 3 h at room temperature. Primary monoclonal antibodies used included: anti-β-galactosidase (1:100; University of Iowa Developmental Studies Hybridoma Bank [DSHB]), anti-Armadillo (1:100; DSHB), anti-β-tubulin (1:50; DSHB), anti-HTS-RC (1:100; Hts 655 4C) and anti-Kelch (1:10; 1B), the latter two gifts from L. Cooley. Secondary antibodies used were Oregon Green or Texas Red-conjugated anti-mouse or anti-rabbit IgG (Molecular Probes). Phalloidin staining was achieved by dissolving 2 units of either Texas Red or Oregon Green-conjugated phalloidin (Molecular Probes) in 200 ml PBT + BSA and incubating for 30 min at room temperature. Phalloidin conjugates were removed by rinsing three times for 15 min in PBT. Labeled preparations were mounted in Vectashield (Vector Laboratories). In order to label nuclei with propidium iodide, tissue preparations were incubated in 125 mg/ml RNase (Boehringer Mannheim) in PBT for 1 h after incubation with secondary antibodies. Preparations were then mounted in Vectashield containing propidium iodide (Vector Laboratories).

2.5. TUNEL labeling

Terminal deoxynucleotide transferase (TdT)-mediated dUTP-biotin nick end-labeling (TUNEL) was performed according to Gavrieli et al. (1992) with minor modifications. Ovaries were placed in a dissection slide and fixed with a 1:1 solution of fix:heptane (fix: 4% paraformaldehyde in PBS) for 20 min with agitation. The preparation was washed three times in PBT and incubated in PBT overnight at 4°C. This was followed by digestion with 2 mg/ml proteinase K (Boehringer-Mannheim) at 25°C for 15 min. The preparation was washed three times in PBT then incubated in 2% H_2O_2 in methanol at 25°C for 15 min. This was followed by a wash in TDT buffer (30 mM Tris [pH 7.2], 0.024% $CoCl_2$, and 30 mg/ml sodium cacodylate) and incubation in the TdT reaction mix (15 μM dUTP, 7.5 μM biotin-dUTP, and 25 U TdT in TdT buffer) at 37°C for 1 h. The preparation was incubated in TB solution (300 mM NaCl and 30 mM sodium citrate) at 25°C for 15 min and blocked in 10 mg/ml BSA in PBS at 25°C for 15 min. This was followed by incubation in 1:50 avidin-horseradish peroxidase (Zymed Laboratories) at 25°C for 45 min and in situ detection of peroxidase using diaminobenzidine (Sigma). The preparation was mounted in 50% glycerol/PBS.

2.6. DAPI, Feulgen, and β-galactosidase staining

Nuclei were labeled with the fluorescent dye DAPI by incubating preparations in 0.2 mg/ml DAPI in PBT for 30 min. Feulgen staining was performed by a modification of an earlier procedure (Galigher and Kozloff, 1971). Ovaries were dissected in PBS, followed by fixation in Carnoy's solution (1:4, acetic acid: ethanol) for 2–3 min. The preparation was then washed in PBS and incubated in 1 N HCl for 3–4 min. After a brief wash in PBS, 1% basic Fuchsin stain was added and the preparation was incubated until the nuclei were appropriately stained. Staining was halted by incubation in dilute sulfuric acid, followed dehydration in a sequence of 10%, 25%, 75%, 100% ethanol. The preparation was cleared with xylene and mounted in permount.

To examine β-galactosidase expression in situ, gonads were dissected in PBS, then incubated in 1:1 fixative: heptane for 20 min with agitation in a covered depression slide with agitation from a rotary shaker for 3 min. The

tissue was rinsed three times in PBT. Staining solution was added and the tissue incubated overnight at room temperature. After staining, the preparation was washed for 20 min five times with PBS. The tissue was mounted in 50% glycerol in PBS. The stock solutions used for this procedure were: Solution A, 6.75 g/l NaCl, 6.63 g/l KCl, 0.66 g/l $MgSO_4 \cdot 7H_2O$, 0.54 g/l $MgCl_2 \cdot 6H_2O$, 0.33 g/l $CaCl_2 \cdot 2H_2O$; Solution B, 1.4 g/l Na_2HPO_4, 0.1 g/l KH_2PO_4, pH 7 (with NaOH); and Solution C, Solution A in 3.7% formaldehyde. The fixative was made up by mixing nine parts of Solution C with 10 parts of solution B. The staining solution consisted of (for a 1 ml volume) 0.75 ml of 9:10 mix of Solution A: Solution B, 0.1 ml 50 mM potassium ferricyanate, 0.1 ml 50 mM potassium ferrocyanate, 50 μl of 100 μg/μl 5-bromo-4-chloro-3-indoxyl-β-galactopyranoside (X-Gal) in *N*,*N*′-dimethylformamide.

2.7. Microscopy

Confocal images were obtained on a Nikon Optiphot using a Bio-Rad MRC 1024 confocal laser apparatus. Sections were manipulated using Bio-Rad Lasersharp image analysis software and transferred to Adobe Photoshop 4.0 for figures. Other microscopy was performed on an Olympus Vanox AHBT3 microscope using an Optronics LX450A camera for image capture.

3. Results

3.1. Construction of transgenes to induce or suppress apoptosis

To study apoptosis in the ovary, we used the yeast *Gal4/UAS* transcription expression system as modified for *Drosophila*. Sequences containing the coding regions of the *rpr*, *hid*, and baculovirus *p35* products were fused to yeast *UAS* regulatory elements and introduced into flies by *P*-element germline transformation. Each construct was first tested for their apoptotic function by examining expression in adult eyes. Previous studies demonstrated that ectopic expression of *rpr* or *hid* resulted in the loss of eye tissue through the induction of apoptosis, while the simultaneous expression of *p35* suppressed this cell death phenotype (White et al., 1994; White et al., 1996; Grether et al., 1995). We induced eye-specific expression from each transgene by *GMR-Gal4*, a construct expressing GAL4 protein in developing eyes. We found that flies with one copy of *GMR-Gal4* and one copy of *UAS-rpr* or *UAS-hid* displayed little to no adult eye tissue, while the addition of *UAS-p35* prevented this cell death from occurring (data not shown). These data demonstrate that *UAS-rpr*, *UAS-hid*, and *UAS-p35* express functional products when in the presence of a GAL4 source.

3.2. Clonal lacZ expression by the 'flip out' technique only occurs in the soma

In order to induce cell death in the ovary without causing organism lethality, a modification of the yeast *FRT-FLP* recombinase system was used (the 'flip-out' technique; Struhl and Basler, 1993). For this method, we required the *Act* > *CD2* > *Gal*4 construct, where expression of GAL4 from the *actin 5C* promoter is blocked by the presence of the *CD2* transcriptional stop sequence (Pignoni and Zipursky, 1997). Two *FRT* sequences flank the *CD2* insert, and are oriented such that site-specific recombination between them leads to the loss of the stop sequence. The recombinant product is an activated *Act* > *Gal*4 derivative capable of constitutive GAL4 expression. *FRT*-specific recombination was mediated by the yeast *FLP* recombinase, originating from a transgene (*hs-FLP*) whose expression is controlled of the *hsp70* heat shock promoter (Golic and Lindquist, 1989). The induction of *FLP* expression by our heat shock regimen leads to formation of GAL4 expressing cells at variable frequencies. The ultimate size of the GAL4-positive clones will depend on the mitotic activity of the affected cells from the time of clonal induction.

Adult female flies carrying one copy each of *hs-FLP*, *Act* > *CD2* > *Gal*4, and *UAS-lacZ* were heat-shocked and their ovaries examined at different time points for β-galactosidase expression (as a marker for GAL4-expressing cells). When examined 12–18 h post-heat shock, follicle cell clones were detected in the egg chambers of all ovarioles examined ($n = 25$ ovaries). Most prominent were small clusters of <5 β-galactosidase-positive cells commonly found in the follicle layer of stage 8 and later chambers (Fig. 1A). These clones must have been induced before the cessation of follicle cell divisions, which occurs during stage 6 (Spradling, 1993).

Isolated β-galactosidase-expressing cells were also detected in previtellogenic egg chambers (Fig. 1A, arrow), indicating clonal induction at these stages but no subsequent mitotic division (as yet). The relatively low β-galactosidase expression levels in these cells compared to stage 8 follicle clones probably reflects their smaller size and the fact that follicle cells in vitellogenic chambers become polyploid (Spradling, 1993), which increases the number of copies of *Act* > *Gal*4 and *UAS-lacZ* in each cell. After 24 h post-heat shock, clones were typically expanded 2- to 3-fold, with the largest clusters found in region 2 of the germarium and in later chambers (Fig. 1B). By 48 h post-heat shock, multi-cell clones were detected during all oogenic stages in over 90% of egg chambers, with particularly extensive patches (representing overlapping clones) in older chambers (Fig. 1C). These observations indicate that the somatic follicle cells are sensitive to *FLP*-induced recombination and GAL4 transcriptional activation during most oogenic stages, beginning in the germarium.

Three observations from these experiments were critical to this study. First, there were no deleterious effects on

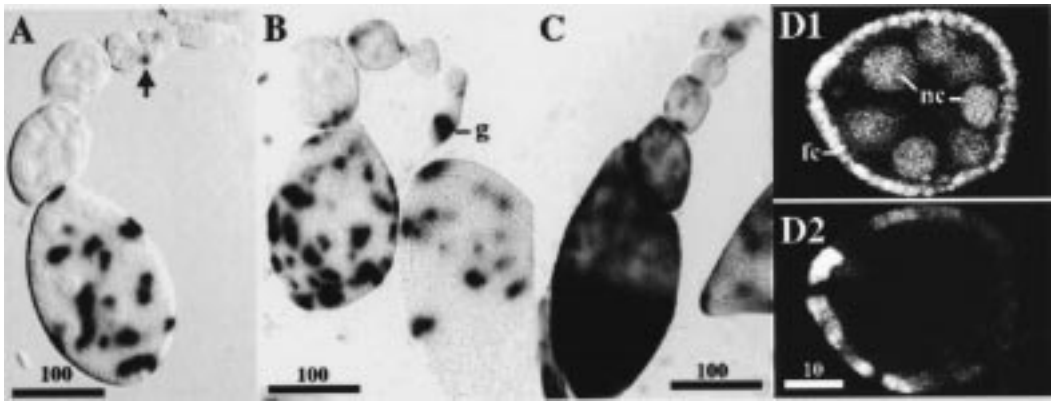

Fig. 1. GAL4 expression induces *UAS-lacZ* expression in the follicle cells but not in the germline. Ovaries are of the genotype *Act* > *CD2* > *Gal4*/+; *UAS-lacZ/hs-FLP* stained for β-galactosidase activity (dark stain). (A) Ovarioles 12–18 h post-heat shock. Arrow points to single cell clone. (B) Ovarioles 24 h post-heat shock. g, germarium. (C) Ovarioles 48 h post-heat shock. (D) Egg chamber stained with propidium iodide and labeled with fluorescently tagged anti-β-galactosidase. (D1) The Texas Red channel shows propidium iodide labeling of nuclei. nc, nurse cells; fc, follicle cells. (D2) Oregon Green channel shows β-galactosidase expression in the follicle cells, but not in the germline. (D1–2) are confocal micrographs.

either follicle cell or germline viability resulting from expression of *hs-FLP*, *UAS-lacZ*, or the activated *Act* > *Gal*4 transgenes. Second, even under heat shock induction, the frequency of site-specific recombination was still relatively low, affecting only a minority of cells (Fig. 1A). Since the gonads are the only region of significant cell division in the adult female, we anticipate that large GAL4-positive clones will be limited to the egg chamber. For this reason any oogenic phenotypes obtained in these experiments will most likely be due to clones induced in the ovaries, rather than to aberrations in other parts of the fly. Finally, we confirm that the UAS/GAL4 system used did not allow induction of gene expression in the germline. Immunohistochemical analyses using antibodies for β-galactosidase failed to detect *UAS-lacZ* expression in germ cells during any oogenic stage, even in cases where substantial portions of the follicle layer were β-galactosidase-positive (Fig. 1D1–2). This inactivity in the germline is consistent with previous observations (Brand and Perrimon, 1993), and is a property of the UAS sequence and 3′UTR used in this experiment (Rorth, 1998).

3.3. rpr and hid can induce apoptotic death in follicle cells

We next tested whether the ectopic expression of *rpr* or *hid* could induce apoptotic death in the somatic follicle cells. Female flies were constructed carrying one copy each of *Act* > *CD2* > *Gal*4, *hs-FLP*, *UAS-lacZ* and either *UAS-rpr* or *UAS-hid*. In these genotypes, GAL4 expressing clones will simultaneously induce *rpr* or *hid* together with *lacZ* expression. When examined 12–18 h after heat-shock, β-galactosidase-positive clones were small and the majority (> 80%) of follicle cells had normal nuclear morphology as observed with the DNA-specific fluorescent dye, DAPI (Fig. 2A). However, an occasional cell displayed nuclear condensation, an early phenotype associated with apoptotic death. By 24–30 h post-heat shock, the frequency of cell death was much higher (Fig. 2B). This was best seen in preparations treated with antibodies to β-galactosidase (Fig. 2C). More extensive, and therefore older, clones displayed many aberrant nuclei, indicating that a minimum of 12–24 h is required from the earliest induction of GAL4 expressing clones for the consistent observation of apoptotic phenotypes in follicle cells. Degenerating follicle cells could be observed at all oogenic stages.

The clonal induction of follicle cell death resulted in major pattern disruptions of the follicle layer in later chambers. This was most easily seen in chambers labeled with antibodies for β-tubulin, which is expressed at high levels in the cell cytoplasm (Fig. 2D). When the dying follicle cells underwent nuclear condensation, cytoplasmic β-tubulin declined to near-background levels (Fig. 2E). The use of this molecular marker revealed extensive discontinuities in the follicle layer of mosaic egg chambers at about stage 6 and later stages (Fig. 2F), but not in earlier, previtellogenic chambers (data not shown).

The observed juxtaposition of apoptotic and normal patches indicate that *rpr*- or *hid*-induced follicle cell death is not necessarily disruptive to neighboring viable cells. However, the degree of this cell autonomy is unclear, as β-galactosidase was probably not a reliable marker of clonal induction in these experiments. It is likely that gene expression, including from *UAS-lacZ*, will terminate as cells degenerate, leading to apoptotic cells absent β-galactosidase activity (arrow, Fig. 2C). This would lead to an underestimate of clone size, with the discrepancy increasing with time as more cells degenerate.

3.4. Disruption of the follicle layer leads to stage-specific germ cell death

Given the somatic specificity of GAL4-induced expres-

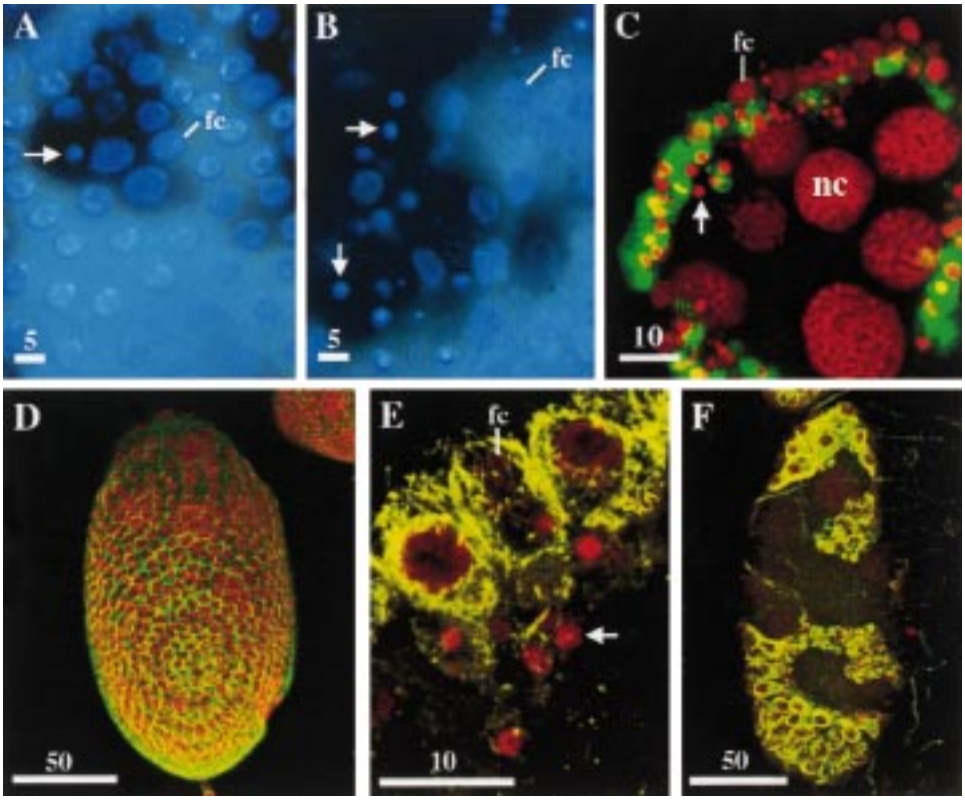

Fig. 2. Expression from *UAS-rpr* or *UAS-hid* induce similar cell death patterns in the follicle layer. Ovaries are of the genotype *Act* > *CD2* > *Gal4/UAS-rpr*; *hs-FLP/UAS-lacZ* (for plates A,B,E,F), *Act* > *CD2* > *Gal4/+*; *hs-FLP/UAS-lacZ*; *UAS-hid/+* (for plates C), or wildtype (plate D). (A,B) Stained for β-galactosidase activity (to identify *rpr*-expressing clones) and DAPI. (A) Follicle cell nuclei (fc) 12–18 h post-heat shock. *rpr*-expressing clones are noted by dark staining. A single condensed nucleus is present in an otherwise normal clone (arrow). (B) Follicle cell nuclei (fc) 24–30 h post-heat shock. Majority of the clone shows nuclear condensation (arrows). (C) Previtellogenic chamber stained with propidium iodide (Texas Red channel) and for β-galactosidase activity (Oregon Green) 24–30 h post-heat shock. Many condensed follicle cell nuclei are present (arrow), including some not associated with β-galactosidase expression. However, nurse cell nuclei appear normal (nc). Similar chambers were found with *UAS-rpr*. (D–F) Stage 7–8 chambers stained for β-tubulin (Oregon Green) and propidium iodide (Texas Red channel). (D) Wildtype egg chamber and follicle layer. (E) High magnification view of viable and inviable follicle cells (fc) from chamber with *rpr*-expressing clones examined 24–30 h post-heat shock. Degenerating follicle cells with condensed nuclei do not express β-tubulin (arrow). (F) Stage 7 chamber 24–30 h post-heat shock. Large discontinuities in the follicle layer are apparent.

sion, an unexpected phenotype was observed 24–30 h after heat shock treatment. Every ovary examined ($n = 50$) contained a variable number of egg chambers with degenerating nurse cells (Fig. 3A,C). This phenotype was stage-specific, affecting only egg chambers at stages 7-8 or later (Fig. 3A,B), and was always associated with degenerating follicle cells ($n = 100$ chambers examined). Nurse cell nuclear condensation was not observed in younger chambers even in the presence of large clones of GAL4-expressing cells (Fig. 2C). In over 25 ovary lobes examined containing chambers with large patches of dying follicle cells, none showed evidence of germline degeneration before stage 7.

This stage specificity was particularly evident in studies examining chromosome integrity. We tested for the occurrence of DNA fragmentation, a characteristic of many apoptotic cells, in the mosaic egg chambers using TUNEL analyses (Gavrieli et al., 1992). Patches of TUNEL-positive follicle cells were observed in previtellogenic and vitellogenic egg chambers, consistent with the continuous sensitivity of the follicle layer to *rpr*- or *hid*- induced apoptosis during oogenesis (Fig. 4A1–2). The occurrence of DNA fragmentation in follicle cells correlated with nuclear condensation, as seen by simultaneous DAPI-labeling (arrow, Fig. 4A3). Note that despite the large clone of TUNEL-positive follicle cells, the nurse cells appeared normal in previtellogenic chambers (Fig. 4A4). DNA fragmentation in the nurse cells first became apparent in stage 7 egg chambers (Fig. 4B1). In this case, DNA fragmentation was associated with aberrations in nuclear shape and the formation of irregular chromatin globules, but occurred before nuclear condensation (Fig. 4B2–3).

A consequence of the stage-specific nurse cell death is a phenotype we designate the 'vitellogenic gap'. Mosaic ovaries from flies incubated for longer times (48–72 h) after heat shock treatment, contained chambers from stages 1–7 and stages 13–14, but were largely devoid of representatives from stages 9–11 (Fig. 5A). This contrasts with what is typically observed in wildtype ovaries (Fig. 5B), indicating that the induction of germ cell aberrations foreshadows the rapid elimination of the defective egg chambers.

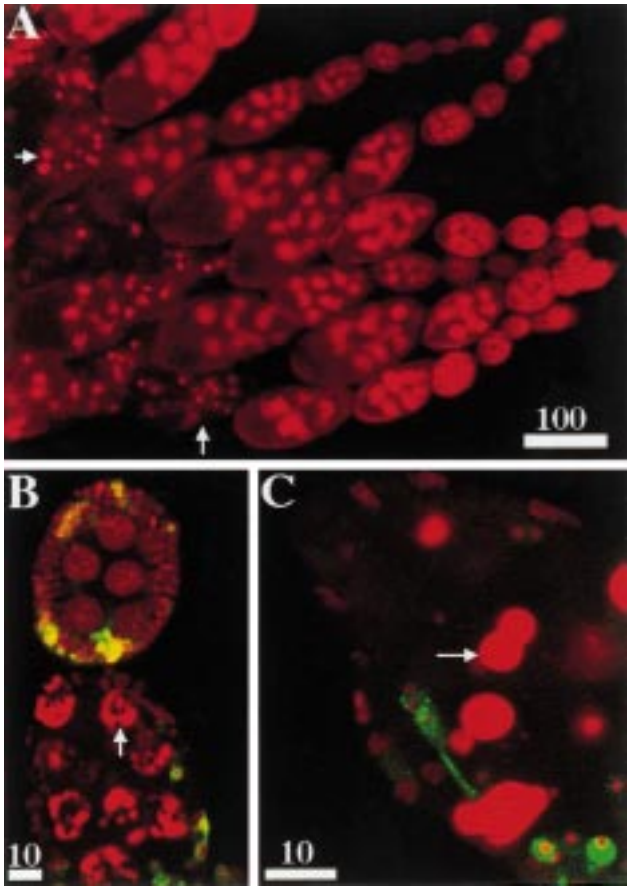

Fig. 3. Follicle cell death leads to stage-specific germline degeneration. Ovaries are of the genotype *Act > CD2 > Gal4/UAS-rpr*; *hs-FLP/UAS-lacZ* (for plate A) or *Act > CD2 > Gal4/+*; *hs-FLP/UAS-lacZ*; *UAS-hid/+* (for plates B, C). (A) Propidium iodide stained ovary examined 24–30 h post-heat shock. Nurse cell degeneration is observed in stage 7 chambers (arrows). (B,C) Confocal images of egg chambers stained with propidium iodide (Texas Red channel) and labeled with fluorescently tagged anti-β-galactosidase (Oregon Green). (B) Two chambers (24–30 h post-heat shock) displaying follicle cell clones expressing β-galactosidase (and *hid*). Upper previtellogenic chamber has normal nurse cells. Lower vitellogenic chamber has aberrant nurse cell nuclei (arrow). (C) An older, more degenerative chamber with condensed nurse cell nuclei (arrow).

3.5. Expression of p35 suppresses follicle cell and germline degeneration induced by rpr

We next examined whether the *rpr*-induced follicle and germline aberrations could be suppressed by the expression of *p35*. This was done to confirm that the follicle cell phenotypes were the result of an apoptotic mechanism, and that the degeneration of the nurse cells was dependent on increased cell death in the follicle layer. Adult females were constructed carrying one copy each of the transgenes *hs-FLP*, *Act > CD2 > Gal4*, *UAS-lacZ*, *UAS-p35*, and *UAS-rpr*. In this genotype, induced clones producing GAL4 will simultaneously express β-galactosidase, *p35*, and *rpr*. GAL4-expressing follicle cell clones were induced by heat shock and examined 24 or 48 h after induction. We found that the mosaic egg chambers ($n > 50$) displayed no morphological aberrations in either the follicle layer or germline after 24–48 h post heat-shock (Fig. 5C, compare with Fig. 3). Even those chambers with multiple clones of β-galactosidase-expressing cells appeared normal (Fig. 5D1,2), with no abnormalities displayed by the GAL4-expressing patches (Fig. 5D3). Based on these results, we conclude that the expression of *rpr* in follicle cells induces a *p35*-sensitive apoptotic pathway. This initiates the degeneration of the germline beginning at about the time of vitellogenesis, ultimately leading to the elimination of the aberrant chamber.

We attempted a similar set of experiments to test interactions between *p35* and *hid*, but were unable to recover flies of the appropriate genotype because of reduced levels of fertility and viability in the preparatory crosses. The reason for this failure is unknown. However, previous studies have shown that *p35* can suppress *hid*-induced apoptosis in other tissues (Grether et al., 1995; Zhou et al., 1997), hence we anticipate the same should be true in follicle cells.

3.6. Nurse cell death initiates with the asymmetric nuclear association of Hts and f-actin

The large size of the nurse cells provides a potentially useful system to examine the cytological events associated with regulated cell degeneration. We performed a series of immunohistochemical experiments to identify some of the molecular events triggered by the stage-specific induction of nurse cell death and to define a time course for these processes. Particularly instructive were our studies with the *hts* gene, which encodes for two products expressed in female germ cells that are critical for oogenesis (Yue and Spradling, 1992; Ding et al., 1993). One Hts protein has homology to vertebrate adducin and is localized to spectrosomes and fusomes, while the other product (HTS-RC) is specific to post-germarial ring canals and probably does not contain the adducin-like domain (Lin et al., 1994; Robinson et al., 1994; Lin and Spradling, 1995).

We examined mosaic ovaries expressing *rpr* 24–48 h post-heat shock. Normally, HTS-RC is localized to the ring canals (Fig. 6A). However, mosaic vitellogenic egg chambers about to degenerate displayed an accumulation of HTS-RC along the nuclear surface of the nurse cells immediately adjacent to the oocyte (arrows, Fig. 6B). This event preceded nuclear condensation, suggesting that HTS-RC might have a nucleus-related function in addition to its role in ring canal morphogenesis (Fig. 6C1). In contrast, the expression of the fusome-specific HTS product was not affected by our experimental manipulations (data not shown). The nuclear attachment of HTS-RC filaments correlated with the elongation and distortion of the nurse cell nucleus (compare Fig. 6C1 with Fig. 6C2).

In every chamber examined ($n = 15$) the HTS-RC product was closely associated with a network of actin filaments (Fig. 6D1–3). Both proteins form preferentially on the most posterior aspect of the nucleus, probably because

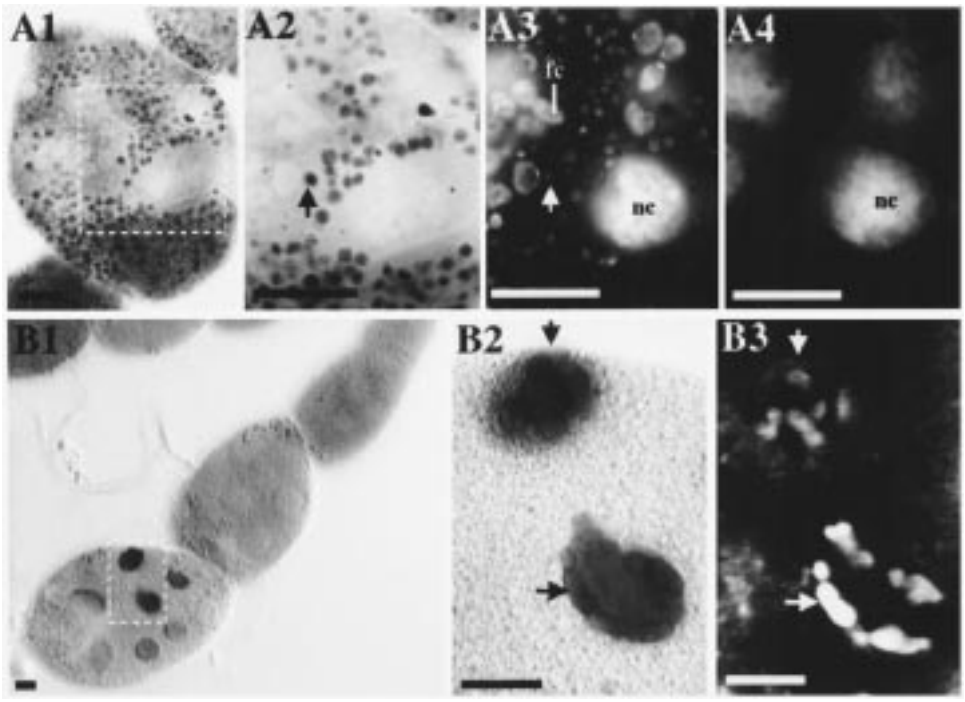

Fig. 4. DNA fragmentation in follicle and nurse cells induced by *rpr*-expression. Chambers are of the genotype *Act* > *CD2* > *Gal4/UAS-rpr*; *hs-FLP/UAS-lacZ* examined 24–48 h post-heat shock. (A) Chamber examined by TUNEL (dark stain) and DAPI (fluoresces under ultraviolet radiation). (A1) TUNEL-labeling of follicle cells (dark stain). Dotted box indicates region magnified in A2–4. (A2) Higher magnification view of portion of (A1). Arrow points to one example of a TUNEL-positive follicle cell. (A3–4) Same section as (A2) but viewed with the ultraviolet channel showing DAPI fluorescence. Different planes of focus are presented. (A3) The image is focused on the outer follicle layer indicating that TUNEL-negative follicle cells (fc) have normal, uncondensed nuclei. Arrow points to location of the TUNEL-positive follicle cell in (A2). (A4) The image is focused on the nurse cells. All nurse cell nuclei appear normal. (B1) TUNEL-positive germ cells first become detectable in stage 7. Dotted box indicates region magnified in B2–3. (B2) TUNEL-positive nurse cell nuclei (arrows). (B3) DAPI-staining shows that TUNEL-positive nurse cells have condensed chromatin (arrows). Size bars equal 10 μm.

of their emanation from the ring canal connecting the nurse cell and oocyte (Fig. 6B,D). HTS-RC and f-actin could also be found along the nuclei of more anterior nurse cells, although typically later than its initial appearance posteriorly (data not shown). Although consistently observed, this anterior association was less obvious and more transient. In fact, the pattern of expression was sufficiently variable that we could not conclusively determine whether these anterior nuclei also displayed asymmetry in the distribution of HTS-RC and f-actin. The nuclear association of HTS-RC and f-actin was followed by DNA fragmentation, with the TUNEL positive chromatin condensing into distinct, often discontinuous segments (Fig. 4B3). By the time of these chromatin changes, the HTS-RC and f-actin filaments have largely disappeared from the nuclear surface of the affected nurse cell.

3.7. Cytoplasmic abnormalities in dying germ cells

The DNA fragmentation coincided with a series of cytoplasmic aberrations affecting the integrity of the nurse cells. This included a sharp reduction in the levels of cortical actin in the nurse cells (compare cortical actin [ca] in Fig. 6D2 with Fig. 6E,F), that contrasted with the relatively high f-actin levels persisting along the inner boundary of the follicle layer (Fig. 6E). A significant decrease also occurred in the levels of *Drosophila* β-catenin, encoded by the *armadillo* (*arm*) gene. In the egg chamber, ARM protein is present in the periphery of the follicle cells and germline during most oogenic stages (Peifer et al., 1993). When follicle cells were induced to die by *rpr* expression, there was a decline in ARM to background levels occurring coincident with nuclear condensation (Fig. 6G). In the germline, a similar reduction in ARM levels occurred simultaneously with the first signs of chromatin abnormalities (Fig. 6H).

Consistent with an apoptotic mechanism, we found that the induced degeneration of the nurse cells stimulated phagocytic activity in the surrounding follicle layer. This was seen by the large fragments of chromatin debris incorporated in a number of somatic cells (arrow, Fig. 6E). Occurring simultaneously with these events were deformities in the morphology of the ring canals. In wildtype egg chambers, the ring canals have a clearly defined shape, as outlined by antibodies to the product of the *kelch* gene (Fig. 6I), and also observed with markers for f-actin and HTS-RC (data not shown). In degenerating nurse cells at about the time of DNA fragmentation (which correlates with the globular nuclear staining pattern, see Fig. 4B), the ring canals became collapsed and misshapen (Fig. 6J,K). By the time the nurse cell nuclei had completely condensed, little germ-

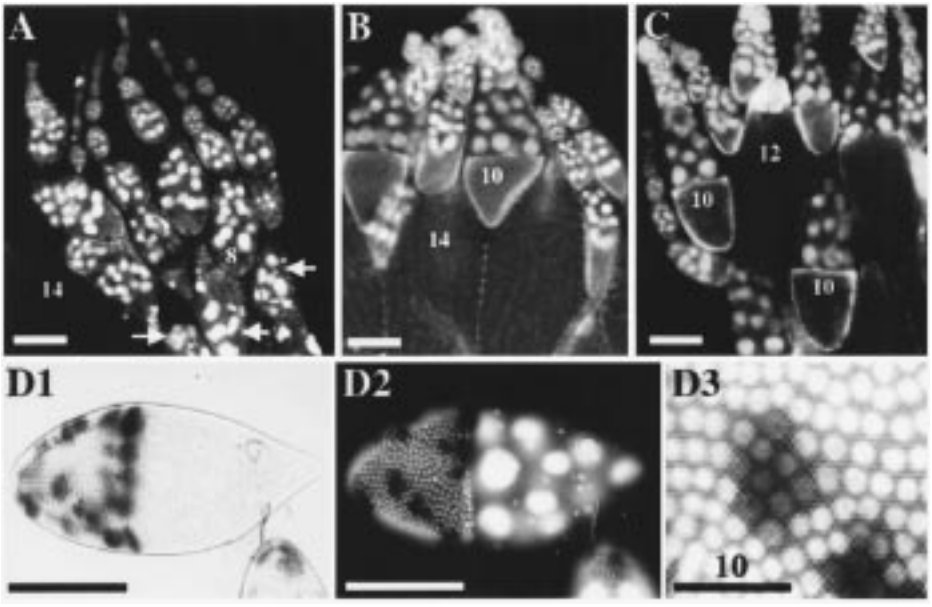

Fig. 5. *p35* expression can suppress the follicle cell and germline death induced by *rpr*. (A) Ovary of the genotype *Act* > *CD2* > *Gal4/UAS-rpr*; *hs-FLP/UAS-lacZ* examined 48–72 h post-heat shock and labeled with DAPI. Numbers indicate oogenic stages. Arrows point to degenerating chambers. Chambers from stages 9–11 are typically absent. (B) Wildtype ovary labeled with DAPI showing stage 10 chambers. The ovary is of the same age (3–7 days) as that shown in (A) and (C). (C) Ovary of the genotype *Act* > *CD2* > *Gal4/UAS-rpr*; *hs-FLP/UAS-lacZ*; *UAS-p35/+* examined 24–48 h post-heat shock and labeled with DAPI. The phenotype is indistinguishable from wildtype. Ovaries of this genotype examined 48–72 h after heat shock were also like wildtype (data not shown). (D) *Act* > *CD2* > *Gal4/UAS-rpr*; *hs-FLP/UAS-lacZ*; *UAS-p35/+* stage 10 chamber examined 24–48 h post-heat shock and stained with DAPI and for β-galactosidase activity (dark stain). (D1) Bright field image showing presence of β-galactosidase expressing follicle cell clones around the oocyte. (D2) Ultraviolet channel showing follicle cell and nurse cell nuclei. (D3) Higher magnification view of portion of follicle layer. DAPI stained nuclei in β-galactosidase expressing clones appear normal. For all figures except D3, size bar equals 50 μm. In D3, size bar equals 10 μm.

line cytoskeletal organization remained, and large pools of cytoplasmic actin were often present in the egg chamber cavity (arrow, Fig. 6F).

3.8. Dying wildtype nurse cells show similar phenotypes

We compared the above phenotypes with those observed in nurse cells dying as a normal consequence of oogenesis. During stages 10–12, the nurse cells deposit their cytoplasmic contents into the oocyte and undergo rapid degeneration by a mechanism that includes nuclear condensation and DNA fragmentation (Foley and Cooley, 1998). We found these apoptotic events were preceded by an association of HTS-RC and f-actin along the nurse cell nuclear surface, reminiscent to that described in our clonal analysis experiments (Fig. 7A, compare with an early, pre-dumping stage 10 chamber in Fig. 6A). However, this phenotype differed in two important respects. First, while there was clear asymmetry in the distribution of the cytoskeletal filaments, there was no preference for an association with any particular side of the nucleus (Fig. 7A,B). Second, we found no consistent difference in the timing of when anterior and posterior nurse cells initiated cell death. Interestingly, in these chambers the HTS-RC and actin filaments tended to be concentrate in regions of nuclear surface infolding (Fig. 7C). A similar phenotype was also seen in our *rpr*-induced degenerating chambers (data not shown).

We also examined the nurse cell phenotypes of wildtype egg chambers that spontaneously degenerate during stages 7–8, presumably in response to defects in oogenic development (Giorgi and Deri, 1976). It was proposed that this phenotype reflects an active mechanism to abort aberrant egg chambers so as to recycle macromolecules and prevent the blockage of the ovarioles. The frequency of such events tended to increase in older females and with more crowded culture conditions (data not shown). We found that such 'stressed' ovaries occasionally contained stage 7–9 chambers displaying the identical HTS-RC and f-actin phenotypes observed in our *rpr* experiments. The frequency of these chambers was variable, but typically at least one was found per ovary lobe. HTS-RC and actin filaments were first and preferentially expressed in the most posterior nurse cells, and were physically associated with the oocyte ring canal (Fig. 7D). Additional similarities were observed in chambers at later stages of degeneration. Coincident with the chromatin condensation and fragmentation, there was a marked reduction in ARM and cortical actin, misshapen ring canals, as well as increased levels of phagocytic activity in the follicle layer (Fig. 7E, data not shown). These phenotypic similarities suggest that the different examples of naturally occurring and experimentally induced, apoptotic-like germline degeneration may utilize the same cell death mechanism.

The formation of a HTS-RC/f-actin network around the

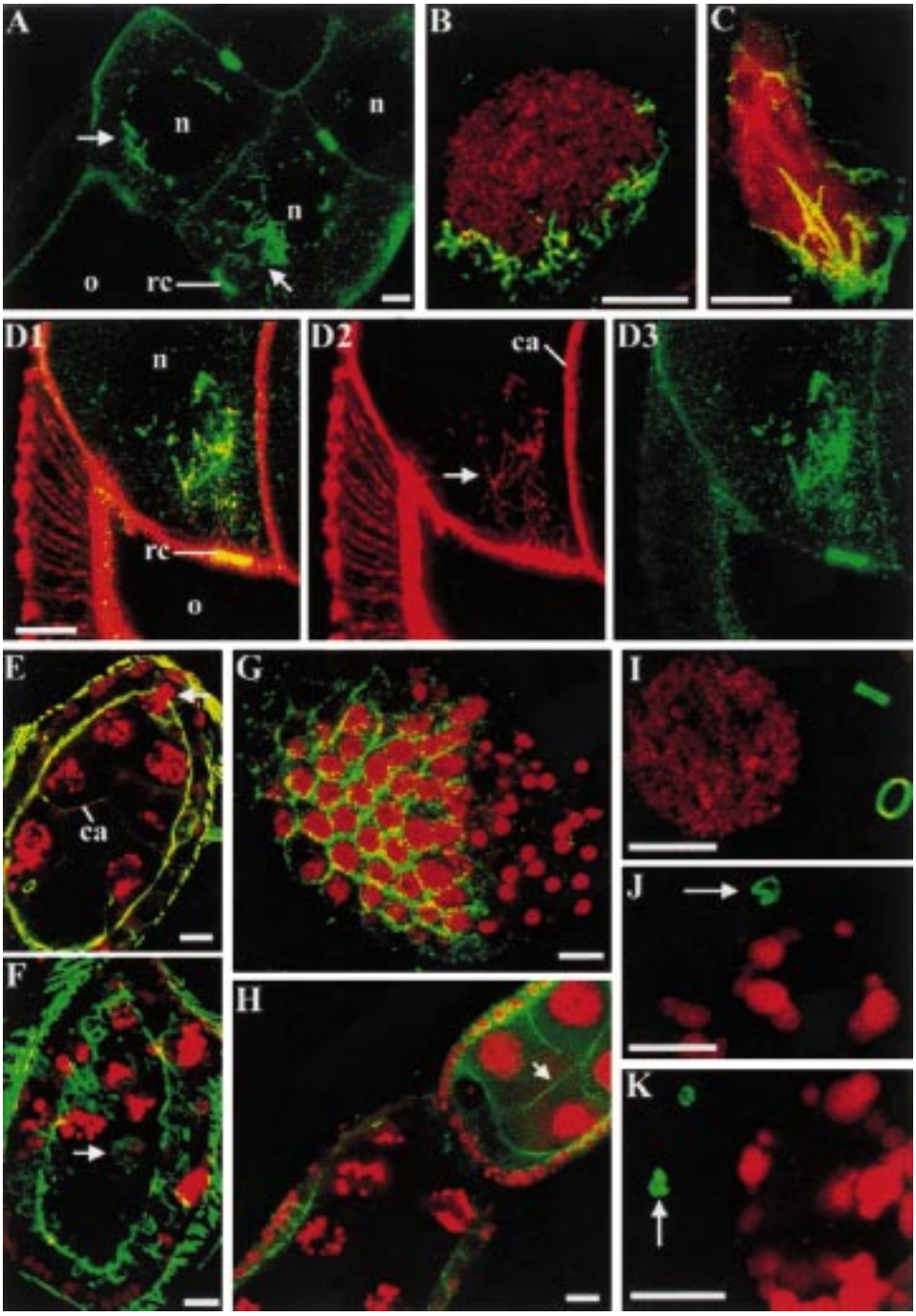

Fig. 6. Cytological events associated with the induced germ cell death. Except for (A), chambers and germ cells are of the genotype *Act* > *CD2* > *Gal4/UAS-rpr*; *hs-FLP/UAS-lacZ* examined 24–48 h post-heat shock. (A) Wildtype stage 10 chamber labeled with anti-HTS-RC (Oregon Green) showing ring canals and no nuclear localization; rc, ring canal. (B) In a *rpr*-expressing mosaic chamber undergoing experimentally induced degeneration, HTS-RC protein (arrow) associates with the nurse cell nuclei (n) closest to the oocyte (o). rc: ring canal. (C) High magnification of two degenerating nurse cell nuclei labeled with propidium iodide (Texas Red channel) and anti-HTS-RC (Oregon Green). (C1) HTS-RC is present on what is otherwise a normal appearing nucleus. (C2) Distorted nucleus associated with HTS-RC. (D1) Nurse cell labeled with anti-HTS-RC (Oregon Green) and phalloidin (Texas Red) showing filaments extending from ring canal (rc) to the nurse cell nucleus (n). (D2) Texas Red channel showing actin filaments (arrow) emanating from the ring canal. Cortical actin (ca) outlines cell bodies. (D3) Oregon Green channel showing HTS-RC filaments overlapping with f-actin. (E,F) Chambers labeled with propidium iodide (Texas Red) and phalloidin (Oregon Green). (E) Note reduced levels of cortical actin (ca) in the nurse cells. Arrow at upper tip points to evidence of phagocytic uptake of condensed chromatin. (F) Further degenerating chamber showing accumulation of actin in cytoplasmic sphere (arrow). (G,H) Chambers labeled with propidium iodide (Texas Red) and anti-ARM (Oregon Green). (G) Follicle cells showing loss of ARM protein in cells with condensed nuclei. (H) ARM protein is present in the nurse cells from normal chambers (arrow) but disappears in later degenerating chambers. (I–K) Nurse cell labeled with propidium iodide (Texas Red) and anti-Kelch (Oregon Green). (I) Wildtype nurse cell nucleus and ring canals. (J,K) Aberrant nurse cell nuclei with aberrant ring canals (arrows). Size bars equal 10 μm. All images are confocal.

nucleus has not previously been observed, suggesting it may be a characteristic specific to germline apoptosis. We tested this possibility by examining mutant egg chambers displaying aborted or aberrant nurse cell differentiation, but no induced germline death. Female flies homozygous for alleles of the germline-specific *ovarian tumor* (*otu*$^{P\Delta 5}$) and *ovo* (*ovo*^{7E}) genes, or the soma-specific small ovaries (*sov*^{2}), *Notch* (*N*^{ts}), and *fs(1)Yb* (*Yb*^{4}) genes, were studied (Oliver et al., 1987; Xu et al., 1992; Geyer et al., 1993; Johnson et al., 1995; Wayne et al., 1995). These alleles allow the differentiation of nurse cells and oocytes, but block egg maturation beginning as early as stage 4. In no case did we observe HTS-RC or f-actin filaments associated with nurse cell nuclei in chambers arrested prior to stage-10 (when nurse cells normally begin to degenerate). HTS-RC was always localized to the ring canals, while f-actin was present in the ring canals and cell periphery (Fig. 7F,G; data not shown). This indicates that the formation of these nuclear-associated

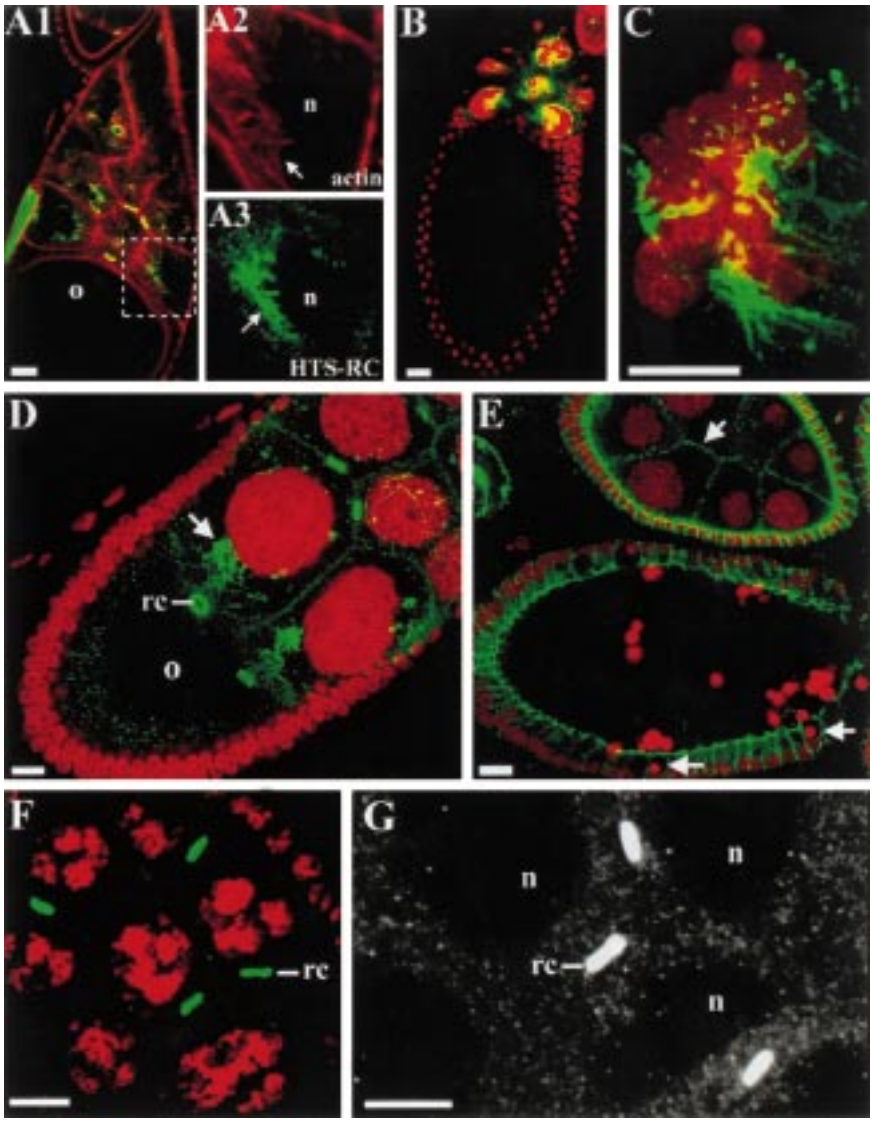

Fig. 7. Cytoplasmic events associated with nurse cell death in wildtype ovaries. (A1) Wildtype chamber from stage 11 labeled with anti-HTS-RC (Oregon Green) and phalloidin (Texas Red); o, oocyte. Box indicates region magnified in A2–3. (A2) Texas Red channel showing actin filaments (arrow). n, nucleus of nurse cell. (A3) Oregon Green channel showing HTS-RC filaments radiating from nucleus (arrow). (B) Stage 11–12 chamber labeled with anti-HTS-RC (Oregon Green) and propidium iodide (Texas Red channel). (C) Nurse cell nucleus from stage 11-12 chamber labeled with anti-HTS-RC (Oregon Green) and propidium iodide (Texas Red channel). (D,E) Degenerating chambers observed in environmentally stressed wildtype ovaries. (D) Stage 8 chamber labeled with anti-HTS-RC (Oregon Green) and propidium iodide (Texas Red channel). On occasions, chambers are observed with HTS-RC filaments (arrow), radiating from ring canal (rc) and associated with nurse cell nuclei. Presumably, these chambers are in the process of degeneration; o, oocyte. (E) Chambers labeled with propidium iodide (Texas Red) and anti-ARM (Oregon Green). ARM protein is present in the nurse cells from normal chambers (arrow) but disappears in lower, degenerating stage 8 chamber with condensed germ line nuclei. In lower chamber, arrows point to evidence of phagocytic uptake in the follicle cells of chromatin debris. (F) *ovo*^{7E} mutant nurse cells (*w ovo*^{7E}/*w ovo*^{7E}) from arrested chamber labeled with propidium iodide (red) and anti-HTS-RC (Oregon Green). (G) *otu*$^{P\Delta 5}$ mutant nurse cells (*y cv otu*$^{P\Delta 5}$/*y cv otu*$^{P\Delta 5}$) from arrested chamber labeled with anti-HTS-RC (Oregon Green). Size bars equal 10 μm. All images are confocal.

networks are specific to the apoptotic germline death process. Similar filaments were not observed in *rpr*- or *hid*-expressing dying follicle cells, however these degenerate so rapidly that short transitional stages would be difficult to detect.

4. Discussion

4.1. Induced apoptosis in the follicle layer leads to stage-specific germline death

The expression of the *Drosophila rpr* and *hid* genes can induce follicle cell degeneration associated with several apoptotic characteristics, including nuclear condensation, DNA fragmentation, and suppression by *p35* expression. This in turn leads to the degeneration of the germline that also displays apoptotic characteristics, including early nuclear condensation, chromatin aberrations, DNA fragmentation, and the stimulation of phagocytic activity in neighboring somatic cells. The degree of follicle cell death required to induce germline apoptosis is variable, but we have observed occasional mosaic chambers with only about 10% of their follicle layer aberrant undergoing germline degeneration (data not shown).

Interestingly, the degeneration of the germline is stage-specific, initiating during stages 7–8. The reason for this temporal specificity likely reflects changes in the biology of the egg chamber that increases its sensitivity to developmental aberrations and apoptotic degeneration. Two factors in particular seem relevant. First, although our clonal technique induced apoptotic follicle cell death during all stages of post-germarial development, it was only in post-stage 6 chambers that large discontinuities in the follicle layer occurred (Fig. 2F). This coincides with the period when follicle cell proliferation ceases, suggesting that prior to this stage the dying cells can be replaced by their proliferative neighbors. Therefore, it may only be in older, nonproliferative chambers that the induced clones produce significant enough damage to the follicle layer to trigger germline death. Second, the *DIAP1* and *DIAP2* (*Drosophila* homologs of baculovirus inhibitors of apoptosis) genes are capable of suppressing *rpr*- and *hid*-induced cell death when expressed in the eye (Hay et al., 1995). Both gene products are found in nurse cells throughout most of oogenesis, potentially providing some resistance to the induction of apoptotic processes (Foley and Cooley, 1998). However, *DIAP1* and *DIAP2* are down-regulated in the germline during portions of stages 7 and 8.

Taken together, these events may make the egg chamber particularly susceptible to pattern disruptions in the follicle layer and the induction of programmed cell death in the germline. This would be consistent with the proposal of Giorgi and Deri (1976) that a mechanism exists for the elimination of aberrant chambers during this period. Support for this comes from the phenotypic similarities in the nurse cell death process observed in the degenerating chambers found in our clonal analysis studies compared to those produced in environmentally stressed wildtype ovaries (Fig. 7D,E). Therefore, our experimentally induced nurse cell death is likely to be a manifestation of a normal process that monitors the fidelity of oogenesis.

We do not know how the disruption of the follicle layer signals the germline to degenerate. Gap junctions linking follicle cells to the nurse cells and oocyte have been observed in stage 4 egg chambers, providing substantial opportunity for intercellular exchange (Giorgi and Postlethwait, 1985). In addition, signaling between the follicle cells and oocyte are known to occur prior to stage 7 for the specification of posterior follicle cells (Gonzalez-Reyes and St Johnston, 1994, 1998; Gonzalez-Reyes et al., 1995, 1997). Hence, follicle cell death during previtellogenic stages will likely disrupt multiple germline-somatic interactions, each potentially contributing to the induction of germ cell death. In this regard, it is interesting to note that ectopic expression of the signaling gene, *wingless*, causes a significant increase in germline degeneration in previtellogenic chambers (Forbes et al., 1996). The reason for this phenotype or the function of *wingless* in oogenesis is not known.

Follicle layer gaps have been reported in egg chambers mutant for elements of the *Notch* and EGF-R signaling pathways (Goode et al., 1992; Xu et al., 1992). These discontinuities result not from follicle cell death, but because of aberrations in cell adhesion or proliferation (Goode et al., 1992). Unlike our clonal analysis results, the *Notch*- and EGF-R-induced follicle disruptions result in fused egg chambers and dorsal-ventral pattern disruptions, rather than germline apoptosis (Xu et al., 1992; data not shown). This difference in phenotype probably reflects the specificity of the *Notch* and *EGF-R* signaling mutations to regulatory pathways associated with a discrete subset of follicle cells. Therefore, the follicle cell gaps produced are relatively small. In contrast, our clonal analysis technique causes a more random and pervasive disruption.

4.2. Cytological events associated with the nurse cell death induced by follicle cell aberrations

Our experimentally induced germline degeneration follows a choreographed sequence of events typical of apoptosis, including DNA fragmentation and other chromatin abnormalities, followed by nuclear condensation and the eventual breakdown of cytoplasmic structures (Fig. 8). However, preceding these apoptotic phenotypes is the transient association of HTS-RC protein along the nurse cell nucleus. While there is no direct evidence that the HTS-RC product directly binds actin, our studies demonstrate a co-localization with actin filaments. The timing of these events suggest that the transient reorganization of the actin and HTS-RC cytoskeleton around the nucleus might play an important role in the subsequent nuclear aberrations associated with apoptotic death. It is noteworthy that the

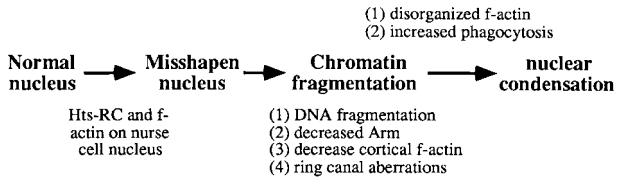

Fig. 8. Sequence of cytological events associated with the induced nurse cell death. The first indication of the nurse cell degeneration is the association of HTS-RC and actin filaments around the nurse cell nucleus. This precedes all other nuclear aberrations. The rearrangement of these cytoskeletal elements is followed by alterations in nuclear shape. At this time, the nucleus-associated HTS-RC and f-actin filaments disappear. Chromatin condensation then occurs, along with DNA fragmentation. Cytoplasmic phenotypes now become apparent, including reductions in the levels of ARM protein and cortical f-actin, and aberrations in ring canal morphology. The final stages of nurse cell apoptosis is associated with nuclear condensation and fragmentation. As this occurs, there is increased phagocytic activity of the surrounding follicle layer, and the pooling of f-actin in the cytoplasm.

same characteristics were observed in nurse cells dying as a normal consequence of oogenesis as well as those found in the occasional degenerating wildtype chambers. This suggests that these divergent cell death phenomenon are occurring by a common mechanism, perhaps specific to the germline.

A curious aspect of this HTS-RC and f-actin network is the temporal polarity of its occurrence with respect to the oocyte. Nurse cells adjacent to the oocyte were the first to display the HTS-RC and f-actin nuclear association, and tended to sustain this interaction for a longer period than more anterior cells. In addition, the f-actin and HTS-RC networks appear to emanate specifically from the ring canals associated with the oocyte, resulting in an asymmetric distribution of fibers along the nuclear surface. Given the normal localization of HTS-RC and f-actin in the ring canals, it is possible that these structures serve as the source of the nuclear filaments. The specific involvement of the oocyte-associated ring canals may indicate a significant function for the oocyte during the initial stages of nurse cell death, perhaps acting as a source of some germline 'death-inducing' signal.

The HTS-RC and f-actin nucleus-associated filaments disappeared at about the time of chromatin condensation and DNA fragmentation. Occurring concomitantly were aberrations in ring canal morphology and the sudden reduction in the levels of ARM (a β-catenin homolog) and cortical f-actin. The degeneration of the egg chamber rapidly followed these events and was associated with the accumulation of cytoplasmic pools of f-actin and the breakdown of nurse cell integrity. Interestingly, both *armadillo* and f-actin have previously been implicated in apoptotic death. The apoptosis-related protease, caspase-3, was shown to cleave β-catenin with possible effects on the actin cytoskeleton (Brancolini et al., 1997). In addition, studies in mammalian cells have suggested that the cleavage of actin might also be associated with certain aspects of cell death (reviewed in Porter et al., 1997), including DNA fragmentation (Villa et al., 1998), although this hypothesis is controversial (see for example; Song et al., 1997; Rice et al., 1998).

In summary, our results demonstrate that aberrations in the integrity of the follicle layer are sufficient to induce stage-specific germline degeneration, indicating that soma-germline interactions are necessary to maintain nurse cell viability. The induced germline death is apoptotic in nature, but is also associated with previously unknown molecular events that may initiate the cell death process. Interestingly, these events are also observed in other instances of germ cell death that occur in wildtype ovaries. This suggests a common cell death mechanism underlying each of these divergent germline death phenomena. Therefore, the nurse cell degeneration induced by our clonal analysis studies is most likely a manifestation of an existing apoptotic process and provides important insights into how this process works.

Acknowledgements

We are grateful to Dr Jeff Denburg and Jan Pettus for helpful discussions and comments. We thank J.M. Abrams, B. Hay, A.H. Brand, L. Zipursky, W. Johnson, K. Golic, L. Cooley and the Bloomington Drosophila Stock Center for clones, fly stocks, and/or antibodies. Some monoclonals were obtained from the Developmental Studies Hybridoma Bank maintained by The University of Iowa, Department of Biological Sciences, Iowa City, IA 52242, under contract NO1-HD-7-3263 from the NICHD. This work was supported by grant GM45843 from the National Institutes of Health and a grant from the Carver Foundation.

References

Ashburner, M., 1989. *Drosophila*, A Laboratory Handbook. Cold Spring Harbor Laboratory Press, Cold Spring Harbor, NY.

Bergmann, A., Agapite, J., Steller, H., 1998. Mechanisms and control of programmed cell death in invertebrates. Oncogene 17, 3215–3223.

Brancolini, C., Lazarevic, D., Rodriguez, J., Schneider, C., 1997. Dismantling cell–cell contacts during apoptosis is coupled to a caspase-dependent proteolytic cleavage of beta-catenin. J. Cell Biol. 139, 759–771.

Brand, A.H., Perrimon, N., 1993. Targeted gene expression as a means of altering cell fates and generating dominant phenotypes. Development 118, 401–415.

Deckwerth, T.L., Johnson Jr, E.M., 1993. Temporal analysis of events associated with programmed cell death (apoptosis of sympathetic neurons deprived of nerve growth factor). J. Cell Biol. 123, 1207–1222.

Ding, D., Parrkhurst, S., Lipshitz, H., 1993. Different genetic requirements for anterior RNA localization revealed by the distribution of adducin-like transcripts during *Drosophila* oogenesis. Proc. Natl. Acad. Sci. USA 90, 2512–2516.

Duke, R.C., Chervenak, R., Cohen, J.J., 1983. Endogenous endonuclease-induced DNA fragmentation: An early event in cell-mediated cytolysis. Proc. Natl. Acad. Sci. USA 80, 6361–6365.

Ellis, R.E., Yuan, J., Horvitz, H.R., 1991. Mechanisms and functions of cell death. Annu. Rev. Cell. Biol. 7, 663–698.

Foley, K., Cooley, L., 1998. Apoptosis in late stage *Drosophila* nurse cells does not require genes within the H99 deficiency. Development 125, 1075–1082.

Forbes, A.J., Spradling, A.C., Ingham, P.W., Lin, H., 1996. The role of segment polarity genes during early oogenesis in *Drosophila*. Development 122, 3283–3294.

Galigher, A.E., Kozloff, E.N., 1971. Essentials of Practical Microtechnique, Lea and Febiger, Philadelphia, PA.

Gavrieli, Y., Sherman, Y., Ben-Sasson, S.A., 1992. Identification of programmed cell death in situ via specific labeling of nuclear DNA fragmentation. J. Cell Biol. 119, 493–501.

Geyer, P.K., Patton, J.S., Rodesch, C., Nagoshi, R.N., 1993. Genetic and molecular characterization of P element-induced mutations reveals that the *Drosophila* ovarian tumor gene has maternal activity and a variable null phenotype. Genetics 133, 265–278.

Giorgi, F., Deri, P., 1976. Cell death in ovarian chambers of *Drosophila* melanogaster. J. Embryol. Exp. Morph. 35, 521–533.

Giorgi, F., Postlethwait, J.H., 1985. Development of gap junctions in normal and mutant ovaries of *Drosophila melanogaster*. J. Morphol. 185, 115–129.

Golic, K.G., Lindquist, S., 1989. The FLP recombinase of yeast catalyzes site-specific recombination in the *Drosophila* genome. Cell 59, 499–509.

Gonzalez-Reyes, A., St Johnston, D., 1994. Role of oocyte position in establishment of anterior-posterior polarity in *Drosophila*. Science 266, 639–642.

Gonzalez-Reyes, A., St Johnston, D., 1998. The *Drosophila* AP axis is polarised by the cadherin-mediated positioning of the oocyte. Development 125, 3635–3644.

Gonzalez-Reyes, A., Elliott, H., St Johnston, D., 1995. Polarization of both major body axes in *Drosophila* by gurken-torpedo signalling. Nature 375, 654–658.

Gonzalez-Reyes, A., Elliott, H., St Johnston, D., 1997. Oocyte determination and the origin of polarity in *Drosophila*: the role of the spindle genes. Development 124, 4927–4937.

Goode, S., Wright, D., Mahowald, A., 1992. The neurogenic locus brainiac cooperates with the Drosophila EGF receptor to establish the ovarian follicle and to determine its dorsal-ventral polarity. Development 116, 177–192.

Grether, M.E., Abrams, J.M., Agapite, J., White, K., Steller, H., 1995. The head involution defective gene of *Drosophila melanogaster* functions in programmed cell death. Genes Dev. 9, 1694–1708.

Hay, B.A., Maile, R., Rubin, G.M., 1997. P element insertion-dependent gene activation in the *Drosophila* eye. Proc. Natl. Acad. Sci. USA 94, 5195–5200.

Hay, B.A., Wassarman, D.A., Rubin, G.M., 1995. *Drosophila* homologs of baculovirus inhibitor of apoptosis proteins function to block cell death. Cell 83, 1253–1262.

Hay, B.A., Wolff, T., Rubin, G.M., 1994. Expression of baculovirus P35 prevents cell death in *Drosophila*. Development 120, 2121–2129.

Hengartner, M.O., 1994. Programmed cell death. A rich harvest. Curr. Biol. 4, 950–952.

Johnson, E., Wayne, S., Nagoshi, R.N., 1995. *fs(1)Yb* is required for *Drosophila* ovary follicle cell differentiation and interacts with members of the *Notch* gene cassette. Genetics 140, 207–217.

Kerr, J., Wyllie, F.R., Currie, A.R., 1972. Apoptosis: a basic biological phenomenon with wide ranging implications in tissue kinetics. Br. J. Cancer 26, 239–257.

King, R.C., 1970. Ovarian development in *Drosophila melanogaster*, Academic Press, New York.

King, R.C., Rubinson, A.C., Smith, R.F., 1956. Oogenesis in adult *Drosophila melanogaster*. Growth 20, 121–157.

Lin, H., Spradling, A.C., 1995. Fusome asymmetry and oocyte determination in *Drosophila*. Dev. Genet. 16, 6–12.

Lin, H., Yue, L., Spradling, A.C., 1994. The *Drosophila* fusome, a germline-specific organelle, contains membrane skeletal proteins and functions in cyst formation. Development 120, 947–956.

Lindsley, D.L., Zimm, G., 1992. The Genome of *Drosophila melanogaster*. Academic Press, Harcourt Brace Jovanovitch, San Diego, CA.

McCall, K., Steller, H., 1997. Facing death in the fly: genetic analysis of apoptosis in *Drosophila*. Trends Genet. 13, 222–226.

McCall, K., Steller, H., 1998. Requirement for DCP-1 caspase during *Drosophila* oogenesis. Science 279, 230–234.

Nordstrom, W., Chen, P., Steller, H., Abrams, J.M., 1996. Activation of the reaper gene during ectopic cell killing in *Drosophila*. Dev. Biol. 180, 213–226.

Oliver, B., Perrimon, N., Mahowald, A.P., 1987. The ovo locus is required for sex-specific germ line maintenance in *Drosophila*. Genes Dev. 1, 913–923.

Peifer, M., Orsulic, S., Sweeton, D., Wieschaus, E., 1993. A role for the *Drosophila* segment polarity gene *armadillo* in cell adhesion and cytoskeletal integrity during oogenesis. Development 118, 1191–1207.

Pignoni, F., Zipursky, S.L., 1997. Induction of *Drosophila* eye development by decapentaplegic. Development 124, 271–278.

Porter, A.G., Ng, P., Jänicke, R.U., 1997. Death substrates come alive. Bioessays 19, 501–507.

Rice, R.L., Tang, D.G., Taylor, J.D., 1998. Actin cleavage in various tumor cells is not a critical requirement for executing apoptosis. Pathol. Oncol. Res. 4, 135–145.

Robinson, D., Cant, K., Cooley, L., 1994. Morphogenesis of *Drosophila* ring canals. Development 120, 2015.

Rorth, P., 1998. Gal4 in the *Drosophila* female germline. Mech. Dev. 78, 113–118.

Song, Q., Wei, T., Lees-Miller, S., Alnemri, E., Watters, D., Lavin, M.F., 1997. Resistance of actin to cleavage during apoptosis. Proc. Natl. Acad. Sci. USA 94, 157–162.

Spradling, A.C., 1993. Developmental genetics of oogenesis. In: Bate, M., Martinez-Arias, A. (Eds.). *Drosphila* Development, Cold Spring Harbor Press, Cold Spring Harbor NY.

Struhl, G., Basler, K., 1993. Organizing activity of Wingless protein in *Drosophila*. Cell 72, 527–540.

Vaux, D.L., Korsmeyer, S.J., 1999. Cell death in development. Cell 96, 245–254.

Villa, P.G., Henzel, W.J., Sensenbrenner, M., Henderson, C.E., Pettmann, B., 1998. Calpain inhibitors, but not caspase inhibitors, prevent actin proteolysis and DNA fragmentation during apoptosis. J. Cell Sci. 111, 713–722.

Wayne, S., Liggett, K., Pettus, J., Nagoshi, R.N., 1995. The genetic characterization of *small ovaries*, a gene required in the soma for the development of the *Drosophila* ovary and the female germline. Genetics 139, 1309–1320.

White, K., Grether, M.E., Abrams, J.M., Young, L., Farrell, K., Steller, H., 1994. Genetic control of programmed cell death in *Drosophila*. Science 264, 677–683.

White, K., Tahaoglu, E., Steller, H., 1996. Cell killing by the *Drosophila* gene reaper. Science 271, 805–807.

Wyllie, A.H., Kerr, J.F.R., Currie, A.R., 1980. Cell death: the significance of apoptosis. Int. Rev. Cytol. 68, 251–306.

Xu, T., Caron, L., Fehon, R., Artavanis-Tsakonas, S., 1992. The involvement of the *Notch* locus in *Drosophila* oogenesis. Development 115, 913–922.

Yue, L., Spradling, A.C., 1992. *hu-li tai shao*, a gene required for ring canal formation during *Drosophila* oogenesis, encodes a homolog of adducin. Genes Dev. 6, 2443–2454.

Zhou, L., Schnitzler, A., Agapite, J., Schwartz, L.M., Steller, H., Nambu, J.R., 1997. Cooperative functions of the reaper and head involution defective genes in the programmed cell death of *Drosophila* central nervous system midline cells. Proc. Natl. Acad. Sci. USA 94, 5131–5136.